05863-14-T

JR.110

THE UNIVERSITY OF MICHIGAN

COLLEGE OF ENGINEERING
DEPARTMENT OF AEROSPACE ENGINEERING
HIGH ALTITUDE ENGINEERING LABORATORY

Technical Report

The Influence of Water Vapor on the Long Wave Stratospheric and Mesospheric Radiation Budget

S. R. DRAYSON and W. R. KUHN

Under contract with:

National Aeronautics and Space Administration
Contract No. NASr-54(03)
Washington, D. C.

Administered through:

December, 1968

OFFICE OF RESEARCH ADMINISTRATION • ANN ARBOR

THE UNIVERSITY OF MICHIGAN

COLLEGE OF ENGINEERING

Department of Aerospace Engineering
High Altitude Engineering Laboratory

Technical Report

THE INFLUENCE OF WATER VAPOR ON THE LONG WAVE STRATOSPHERIC AND MESOSPHERIC RADIATION BUDGET

S. R. Drayson and W. R Kuhn

ORA Project 05863

under contract with

NATIONAL AERONAUTICS AND SPACE ADMINISTRATION

CONTRACT NO. NASr-54(03)

WASHINGTON, D. C.

administered through

OFFICE OF RESEARCH ADMINISTRATION ANN ARBOR

December 1968

This report is the text of a paper presented to the Conference on Composition and Dynamics of the Upper Atmosphere, American Meteorological Society, November 6-8, 1968, El Paso, Texas.

Table of Contents

List of Figures

1. Introduction

Radiative heating and cooling rates are important contributions to an analysis of the atmospheric heat budget. These radiative contributions have been calculated for the troposphere with reasonable accuracy (see e. g. Davis, 1963, Rodgers, 1967) and also for the upper stratosphere and mesosphere (Murgatroyd and Goody, 1958, Kuhn and London, 1968). Although some calculations have included the lower stratosphere, this region has not been of major concern in the previous calculations. One difficulty is the uncertainty in the water vapor concentrations in the atmosphere above the tropopause. Observations extend only to approximately 30 km and the validity of certain of these measurements is still open to question. Recently, Mastenbrook (1968) summarized the water vapor data, and although the lower stratosphere appears, in general, to be dry (mixing ratio $2\text{-}3\text{x}10^{-6}$ gm/gm) there is a general tendency for the concentration to increase with elevation above approximately 30-50 mb. There are also cases for which the mixing ratio increases quite rapidly, reaching a value greater than $2\text{x}10^{-5}$ gm/gm at 15 mb. It is the purpose of this paper to estimate the importance of the 6.3 and 80 μ m bands of water vapor to the lower stratospheric heat budget based upon the recent summary of water vapor distributions by Mastenbrook. We shall also include results of earlier work (Kuhn and London, 1968) for the upper stratosphere and mesosphere.

2. Methodology

The radiative temperature change (hereafter designated as rtc) was evaluated from the expression

$$\frac{\Delta T}{\Delta t} = \frac{g}{c_p} \frac{\Delta F}{\Delta p} \qquad (1)$$

where $\Delta T/\Delta t$ is time rate of change of temperature, g is the acceleration due to gravity, c_p is the specific heat of air at constant pressure p, and F

is the net radiative flux which can be expressed as the difference of an upward ($F^{\uparrow}$) and downward ($F^{\downarrow}$) directed component.

$$F^{\uparrow}(u_o) = \sum_i \delta_i \pi \left[B_i(o)\tau_i(u_o) + \int_o^{u_o} B_i(u) \frac{d}{du} \tau_i(u_o, u) du \right]$$

$$F^{\downarrow}(u_o) = \sum_i \delta_i \pi \int_{u_\infty}^{u_o} B_i(u) \frac{d}{du} \tau_i(u_o, u) du \qquad (2)$$

where u is the mass path, with reference to the earth's surface, B is the Planck function, δ_i is the width of the i^{th} wave number interval, and τ_i is the flux transmissivity (diffusivity factor = 1.667) corresponding to that interval. The summation extends over the i wave number intervals spanning the band.

The transmission function was calculated with the aid of the quasi-random band model (Wyatt et al., 1962). We assumed pure collision broadening (Lorentz profile) below 30 km, and above 30 km a combined collision, Doppler broadening (Voigt profile) was used. The transmission functions for these cases can then be expressed as,

i. Lorentz (Wyatt et al., 1962)

$$\tau_i = \left[\prod_{k=1}^{5} \left\{ \frac{1}{2} \int_{-1}^{1} \exp\left[-\frac{\varphi^2 \xi_k}{(\epsilon' - \eta)^2 + \varphi^2} \right] d\eta \right\}^{n_k} \right] \prod_{\substack{\ell=1 \\ \neq i}}^{j} \left[\prod_{k=1}^{5} \left\{ \frac{1}{2} \int_{-1}^{1} \exp\left[-\frac{\varphi^2 \xi_k}{(\epsilon' - \eta)^2} \right] d\eta \right\}^{n_k} \right] \qquad (3)$$

where,

$\varphi = 2\alpha_L/\delta$, where α_L is the Lorentz halfwidth

$\xi_k = S_k u / \pi \alpha_L$, where S_k is the average line strength for the k^{th} intensity decade within the i^{th} wave number interval.

$\epsilon = 2\frac{(\omega - \omega_o)}{\alpha_L}$, where $\omega - \omega_o$ is the distance from the center (ω_o) of the i^{th} spectral interval.

n_k = the number of lines in the k^{th} intensity decade

The first bracket represents the contribution to the flux transmissivity from spectral lines lying within that spectral interval, while the second bracket contains the contribution to the transmission from the wings of spectral lines lying outside the spectral interval in question.

ii. Voigt (Kuhn and London, 1968) (4)

$$\tau_i = \prod_{k=1}^{5} \left\{ \frac{1}{2} \int_{-1}^{1} \exp\left[- \frac{S_k u a (\ell n 2)^{\frac{1}{2}}}{\alpha_D \pi^{3/2}} \int_{-\infty}^{\infty} \frac{\exp(-y^2)\, dy}{a^2 + \left[(x\delta (\ell n 2)^{\frac{1}{2}} / 2\alpha_D) - y \right]^2} \right] dx \right\}^{n_k}$$

$a = \alpha_L (\ell n 2)^{\frac{1}{2}} / \alpha_D$, where α_D is the Doppler half width

$x = 2(\omega - \omega_o)/\delta$

Calculations of rtc were made for the 80 μ m and 6.3 μm H_2O bands. The 80 μm line strengths and positions are from Benedict (1965) for the spectral interval from 200 to 500 cm^{-1} and from Yamamoto and Onishi (1951) for the interval from 0 to 200 cm^{-1} and 500-600 cm^{-1}. The band parameters for the 6.3μm band are from Wyatt et al (1962). Line strengths correspond to a temperature of 250 K and the surface collision half widths are 0.087 and 0.1 cm^{-1} for the 80 μm and 6.3 μ m bands respectively. No variation of Doppler half width with temperature or wave number was considered, the half widths being $2.66 \times 10^{-4} cm^{-1}$ and $1.56 \times 10^{-3} cm^{-1}$ for the 80 m and 6.3 m bands respectively. Up to 30 km, the spectral interval was 200 cm^{-1} for the 80μm band, the band extending from 0 to 600 cm^{-1}. The 6.3 μm band extended from 1000 to

2400 cm^{-1}, and was divided into three equal spectral intervals. Above 30 km, the spectral intervals for both bands were 25 cm^{-1}. The calculations for elevations above 30 km were made at an earlier date and no larger spectral intervals were studied; however, we found that spectral intervals of 300 and 200 cm^{-1} gave errors of only a few percent in the lower stratospheric rtc.

Transmission profiles for the 80 μm rotational band are shown in Fig. 1. These calculations were made for transmission averages over 25 cm^{-1} intervals. The lower most curve corresponds to an atmospheric layer extending from 7 to 30 km for an equatorial water vapor distribution and a stratospheric mixing ratio of 10^{-4} gm/gm (Kuhn, 1966). As will be shown, the radiative flux from the lower troposphere gives a relatively small contribution to the flux divergence within the stratosphere. Thus rotational lines beyond about 550 cm^{-1} are negligible for these calculations, and a comparison of this transmission function with the 15 μm CO_2 transmission functions (Kuhn, 1966) shows that we may neglect band overlap between the 80 μ m and 15 μ m transitions.

3. Results

Results for the calculations from the data of Mastenbrook (1968) are given in Fig. 2. Profile II corresponds to the median distribution of water vapor for Washington, D. C. and Trinidad, W. I. The maximum distribution (profile III) corresponds to the large mixing ratios found over Trinidad, W. I., for pressure levels of 15-20 mb. Profile I represents the case for which the mixing ratio decreases uniformly with height. The mean temperature distribution which was used for these calculations is also given in Fig. 2.

Calculations were made at approximately 2-3km intervals. For all three cases a slight heating is indicated in the tropopause region. Throughout the lower stratosphere, up to a height of approximately 25 km, the cooling is

a few tenths of a degree per day. Above 25 km, profiles I and II show a cooling which increases to approximately 0.6 deg/day while the rapidly increasing mixing ratio produces a rtc approximately twice as large as the median distribution as given by profile II. While this larger water vapor concentration produces a much larger cooling effect above approximately 26 km, below this elevation the larger H_2O concentration actually causes a smaller cooling than the smaller H_2O distributions. This occurs because of the larger downward flux which compensates the upward flux, which is the primary contributor to the radiative heating. Higher in the atmosphere, however, the downward flux is the major contributor to the rtc, and here the downward flux difference is greater for the larger H_2O concentration than for the smaller concentrations given by II and I.

The dashed curve represents the contribution to the rtc by the 6.3μm band. Near the tropopause both the 6.3μm and 80μm bands produce a heating of similar magnitude; however, the heating by the 6.3μm band decreases rapidly with elevation becoming less than 5 percent of the 80μm cooling at a height of 20km.

Because of the uncertainty in the H_2O concentrations in the upper stratosphere and mesosphere, two extreme concentrations have been assumed (Kuhn 1966), with values of 10^{-4} and 10^{-6}gm/gm, (Fig. 3). Each of these distributions has then been coupled with extreme tropospheric distributions corresponding to equatorial (profile I) and polar (profile II) mixing ratio distributions along with the corresponding temperature profiles. The heavy line refers to the upper atmospheric mixing ratio of 10^{-6}while the light line refers to a mixing ratio of 10^{-4}. The dashed line corresponds to the 6.3μm band for a tropospheric equatorial water vapor distribution and an upper atmospheric distribution of 10^{-4}gm/gm. All other profiles refer to the 80μm band. For an upper atmosphere mixing ratio of 10^{-4}, the rtc by the rotational band is 2-4 deg/day, while a mixing ratio of 10^{-6} produces a cooling less than 1 deg/day.

The contribution of the 6.3 μm band to the rtc is of only minor importance when compared with the rotational band. Near the stratopause where the temperature is high the 6.3 μ m band contributes less than 30 percent as much cooling as does the rotational band ($\sim$3.8 deg/day); for elevations above approximately 55 km and below 45km, the contribution of the 6.3 μ m band is less than 10 percent of the cooling by the rotational band.

Kuhn (1966) has shown that the source function for the 6.3 μm band deviates from the Planck function above approximately 60 km; however, as can be seen the cooling at 60 km is only 0.1 deg/day and is certainly negligible in comparison to the rotational band cooling. Thus non LTE calculations are not required and flux divergence calculations for this band may be made in a straightforward manner as given in eqns (1) and (2). Similarly, the large collisional rates for the 80 μ m transitions insure that the same formulation will hold for this band also (Kuhn, 1966).

Recent estimates by Hesstvedt (1968) indicate that the mixing ratio is approximately 5×10^{-6} gm/gm at 65 km and decreases slowly with elevation, becoming 1.1×10^{-6} at 95 km. Thus the rtc produced by the 80 μ m band is probably about 1 deg/day in the upper stratosphere and lower mesosphere. Above approximately 65 km, the cooling rate is less than a tenth of a degree per day and calculations using the method of Drayson (1967) have shown that above 70 km the rtc by the 80 μ m band is negligible in comparison to the rtc by the 15 μ m CO_2 band (less than a few tenths of a degree per day).

The contributions to the rtc at a particular height from the various atmospheric layers are shown in Fig. 4. The shaded regions represent positive contributions, or heating, to the layer in question, while the unshaded region represents the emission by that layer. The difference between the emission of that layer and the absorption of energy from the adjacent layers

is the rtc which is indicated by the dashed line. The dotted line represents a "cooling to space" term which is one-half the emission of the layer in question. While the actual rtc approaches the "cooling to space" emission as the elevation increases, notice that even at 27.5 km, the cooling to space term is approximately 70 percent larger than the actual rtc.

Only the atmosphere within 8 km above the level in question strongly influences the rtc while the contributions from below extend down to the mid troposphere. Thus the distributions of water vapor and temperature in the lower troposphere do not significantly influence the rtc in the stratosphere.

An approximation to Newtonian cooling is shown in Fig. 5. The rtc for the 80 μ m band was calculated for the mean water vapor distribution (profile II) with temperature profiles selected from the U.S. Standard Atmosphere Supplement, 1966. Expressing the cooling as a linear function of temperature is a poor approximation in the lower stratosphere, up to about 100 mb; however, with increasing elevations, the approximation becomes better, and at 10.4 mb, the fit is excellent. One would expect similar good agreement at higher elevations, although these calculations were not made because of the uncertainty in the water vapor distributions.

4. Conclusions

Although water vapor is not the primary contributor to the infrared rtc in the lower stratosphere, nevertheless, it does make an important contribution, being approximately 50 percent as large as the cooling by the 15 μ m CO_2 band. A strongly increasing mixing ratio will produce a larger rtc in the mid stratosphere (1-2 deg/day) but its effect will be to reduce the cooling by about 0.1 deg/day

in the lower stratosphere. For climatological studies the 6.3 μ m band may be neglected in the stratosphere and mesosphere. The cooling by the 80 μ m band in the stratosphere and mesosphere is probably about one degree per day, although with a very large mixing ratio ($\sim 10^{-4}$ gm/gm), the 80μ m band cooling would be approximately equal to the 15 μ m CO_2 band cooling in the mid stratosphere and mid mesosphere.

A cooling to space or Newtonian cooling approximation is valid for pressures less than approximately 100 mb. At 10.4 mb ($\sim$ 31 km) the linear approximation is excellent.

References

Benedict, W S., 1965: unpublished data.

Davis, P., 1963: An analysis of the atmospheric heat budget. J. Atmos. Sci., 20, 5-22.

Drayson, S. R., 1967: Calculation of long-wave radiative transfer in planetary Atmospheres. PhD Thesis, Univ. of Mich. ORA Report 07584-1-T.

Hesstvedt, E., 1968: On the effect of vertical eddy transport on atmospheric composition in the mesosphere and lower thermosphere. Geophys. Publik., Geophys. Norvegica, 27, No. 1, 1-35.

Kuhn, W. R., 1966: Infrared radiative transfer in the upper stratosphere and mesosphere. Sci. Rep., Nat. Sci. Foun., Atmos. Sci. Section, NSF GP 3196, 159 pp.

Kuhn, W. R., and J. London, 1968: Infrared radiative cooling in the middle atmosphere. (accepted for publication) J. Atmos. Sci.

Mastenbrook, H. J., 1968: Water vapor distribution in the stratosphere and high troposphere. J. Atmos. Sci., 25, 299-311.

Murgatroyd, R. J. and R. M. Goody, 1958: Sources and sinks of radiative energy from 30 to 90 km. Quart J. R. Meteor. Soc., 84, 224-234.

Rodgers, C. D., 1962: The radiative heat budget of the troposphere and lower stratosphere. Report No. A2, Dept. of Meteorology, Mass. Inst. Inst. of Tech., 99 pp.

Wyatt, P. J., et al., 1962: The infrared absorption of water vapor. Final Report, SSD-TDR-62-127-Vol II, Aeronutronic Div., Ford Motor Co.

Yamamoto, G., And G. Onishi, 1951: Appendix to our paper on "Absorption coefficient of water vapor in the far infrared region." Sci. Reps. of the Tohoku Univ., Series 5, Geophysics, 13, 1-8.

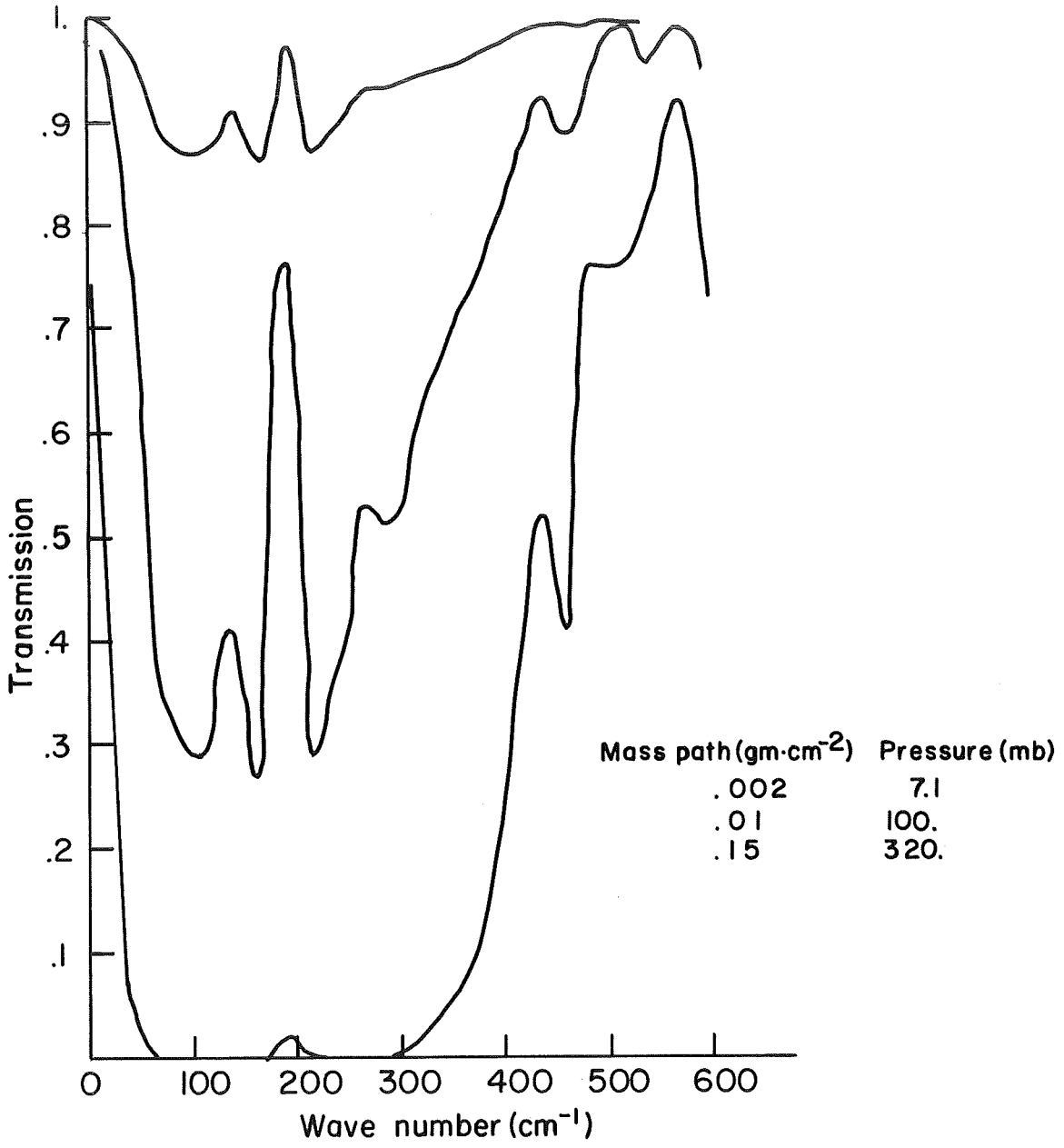

Fig. 1. Flux transmissivities for the 80 μm H_2O band as calculated from the quasi-random model.

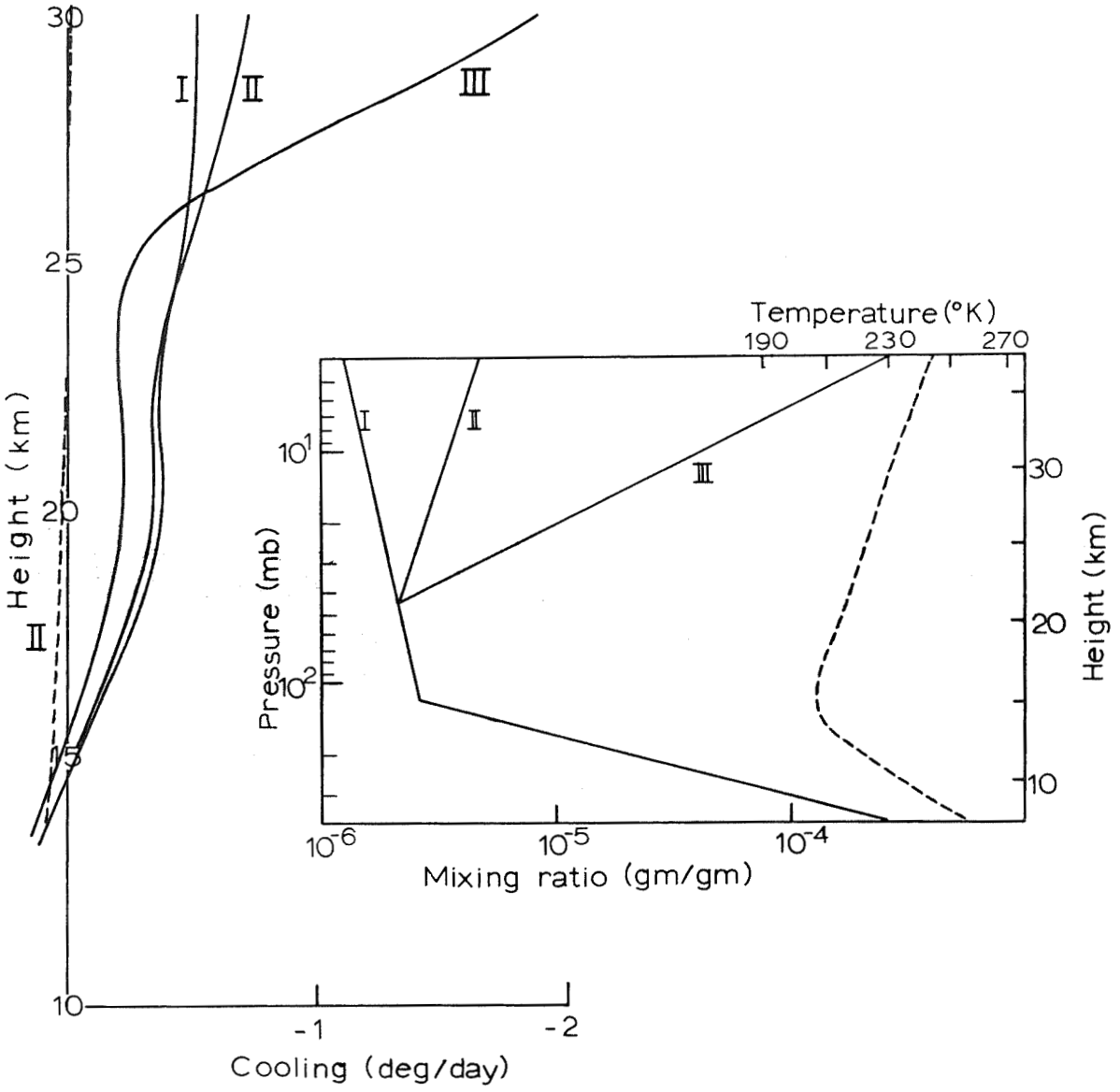

Fig. 2. Stratospheric rtc as produced by the 80 μm and 6.3 μm (dashed) H_2O bands for selected mixing ratio distributions.

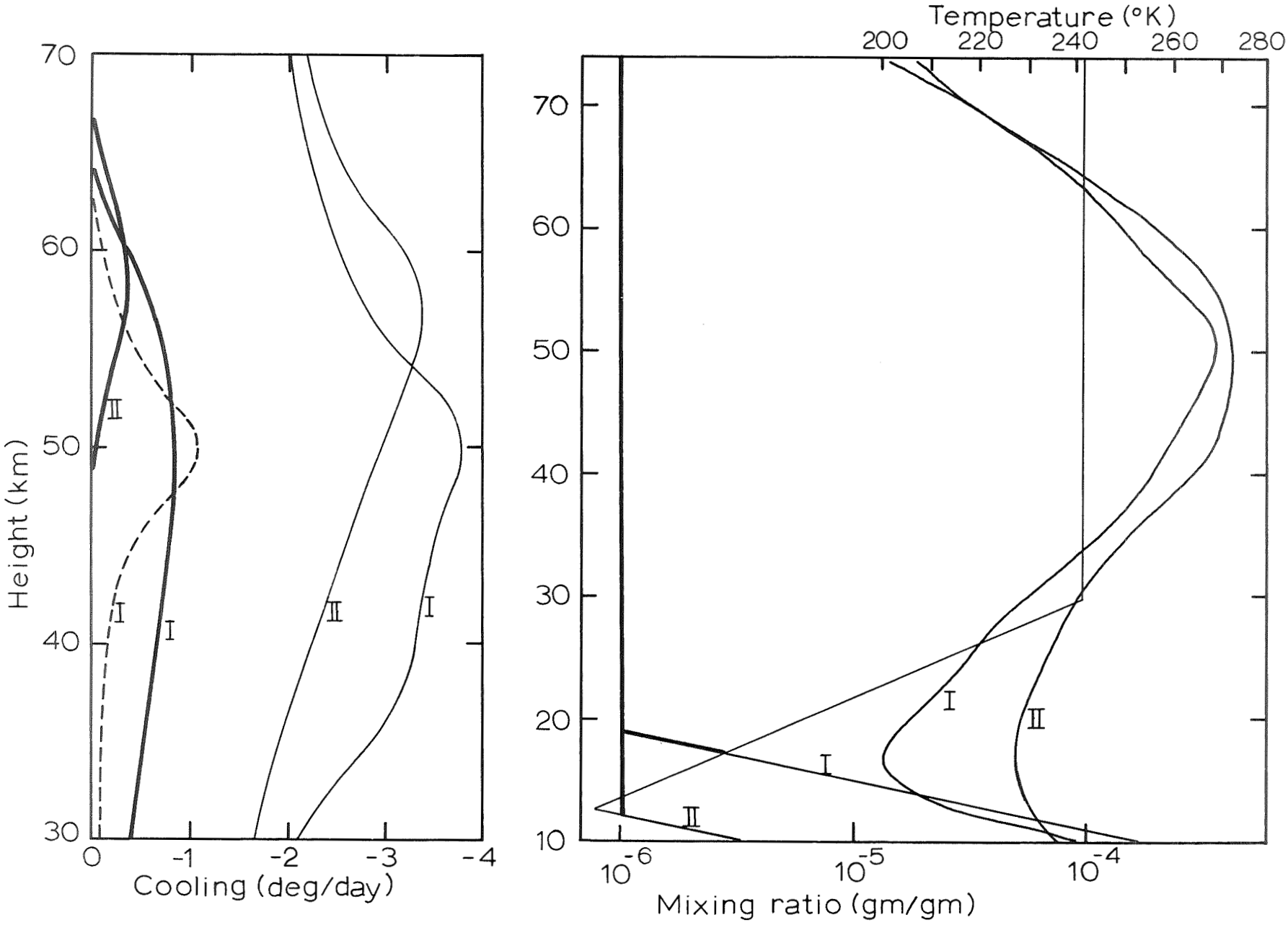

Fig. 3. Upper stratospheric and mesospheric rtc as produced by the 80 μm and 6.3 μm (dashed) H_2O bands for selected mixing ratio and temperature distributions.

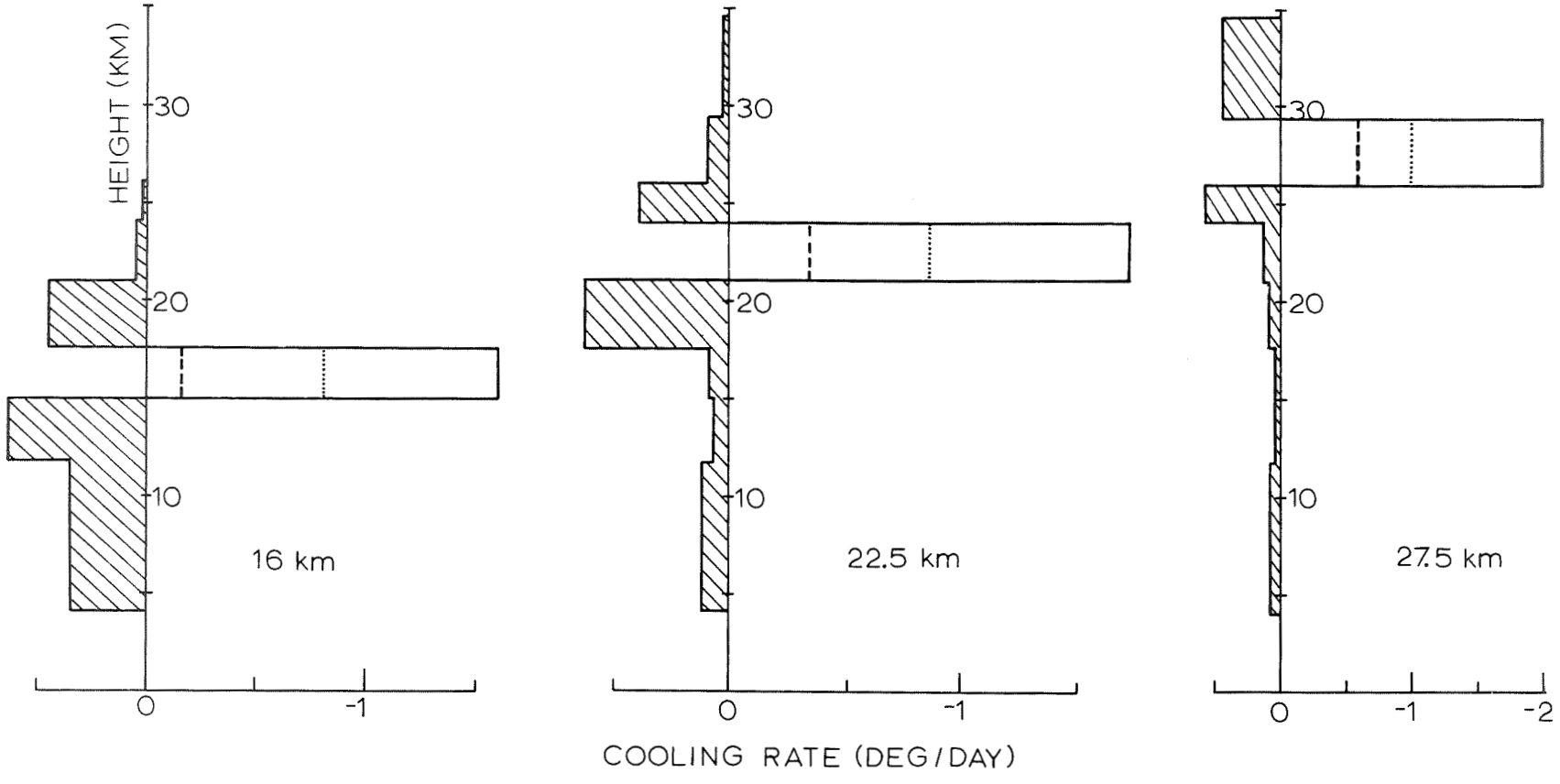

Fig. 4. Contributions to radiative heating (shaded area) and cooling at selected heights from adjacent atmospheric layers. Actual rtc is indicated by the solid vertical line while the "cooling to space" is denoted by the dotted line.

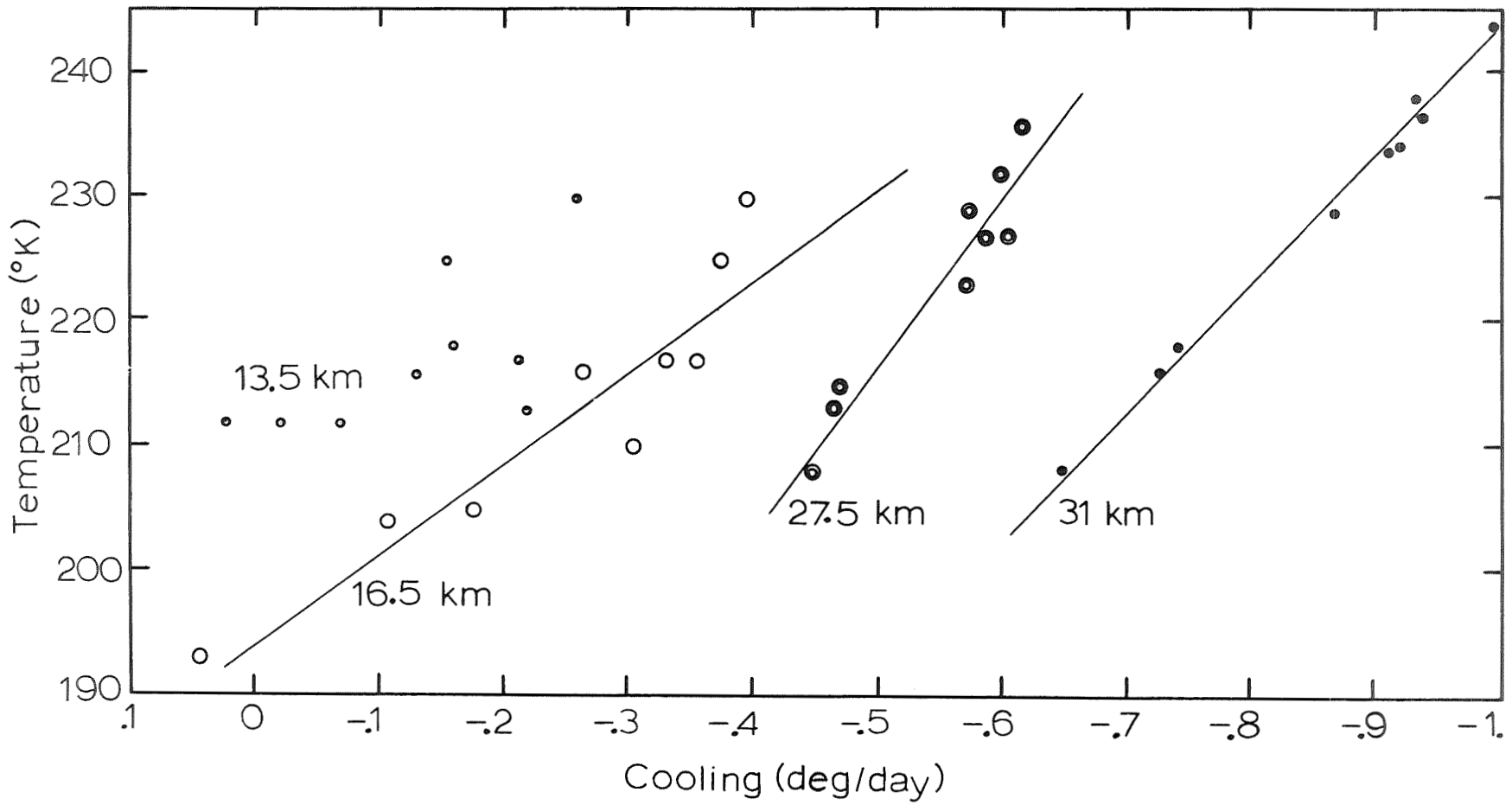

Fig. 5. "Newtonian cooling" approximations at selected stratospheric elevations.